

Asymptotic freedom and the "absence" of vector-gluon exchange in wide-angle hadronic collisions

R. F. Cahalan*[†] and K. A. Geer*[‡]

Department of Physics, Syracuse University, Syracuse, New York 13210

J. Kogut[§] and Leonard Susskind^{||}

Laboratory of Nuclear Studies, Cornell University, Ithaca, New York 14853

(Received 7 October 1974)

The naive, pointlike parton model of Berman, Bjorken, and Kogut is generalized to scale-invariant and asymptotically free field theories. The asymptotically free field generalization is studied in detail. Although such theories contain vector fields, single vector-gluon exchange contributes insignificantly to wide-angle hadronic collisions. This follows from (1) the smallness of the invariant charge at small distances and (2) the breakdown of naive scaling in these theories. These effects should explain the apparent absence of vector exchange in inclusive and exclusive hadronic collisions at large momentum transfers observed at Fermilab and at the CERN ISR.

I. INTRODUCTION

It has long been hoped that the study of processes involving large momentum transfers would reveal the degrees of freedom and the dynamics which underlie strong interactions. Lepton-induced reactions such as deep-inelastic electroproduction and neutrino-induced production have been remarkably productive in this respect. At a more speculative level it has also been suggested that purely hadronic reactions at high momentum transfer should also reveal the fundamentals behind strong interactions. As early as 1965 Wu and Yang¹ suggested that elastic proton-proton scattering at large s and t should share many features in common with elastic lepton-hadron scattering. This suggestion led to many models of inclusive and exclusive hadron-hadron processes involving large momentum transfers.² Most of these models were presumably based upon field theories in which quarks are bound together into hadrons by the exchange of vector gluons. The many reasons for considering such a class of theories need not be repeated here. Suffice it to say that the success of the parton model in describing lepton-induced deep-inelastic reactions has provided additional support for such theories. In this context the Feynman diagram which is expected to produce wide-angle inclusive and exclusive hadron-hadron scattering involves the exchange of a single gluon. Estimates of such processes are easily made and were originally thought to provide a description of the experimental data. However, it has become clear recently that single vector-gluon exchange fails to explain both the angular distribution and energy dependence of the processes of interest.³ Apparently single gluon exchange is *not* the dom-

inant mechanism involved. It is the purpose of this article to suggest why this is the case.

The result comes about in the following way. Consider the theory of colored quarks coupled in a gauge-invariant fashion to colored vector bosons. Let the ordinary symmetry group of strong interactions be SU(3) or SU(4) and let the color group be SU(3)'. Then such a theory is asymptotically free (AF) with an invariant quark-gluon coupling constant,

$$\frac{\bar{g}^2(Q^2)}{4\pi^2} \underset{Q^2 \rightarrow \infty}{\sim} 2 \left(b_0 \ln \frac{Q^2}{\mu^2} \right)^{-1}, \quad (1.1)$$

where μ is a scale parameter and b_0 is a numerical constant depending on the color group.⁴ Furthermore, the structure functions in deep-inelastic leptoproduction violate Bjorken scaling⁵ in a computable fashion: They fall near x of 1 (x is the standard scaling variable of Bjorken⁵) and rise near x of 0 as Q^2 grows. As will be discussed in detail below, the probability for a large momentum transfer to occur between colliding hadrons depends sensitively on the size of the hadron's structure functions near $x=1$. If these functions are small near $x=1$, then the production of high-transverse-momentum secondaries is small. We shall see that two effects, (1) the smallness of $\bar{g}(Q^2)$ for large Q^2 , and (2) the breakdown of Bjorken scaling, cause the production of high-transverse-momentum secondaries through the exchange of a vector gluon to be "negligibly" small. One might have guessed that (2), the breakdown of naive scaling in AF theories, would not be a numerically significant effect. We will see in the text that this is *not* true—numerical estimates show that (2) reduces the production of high-transverse-momentum secondaries by 1 to 2

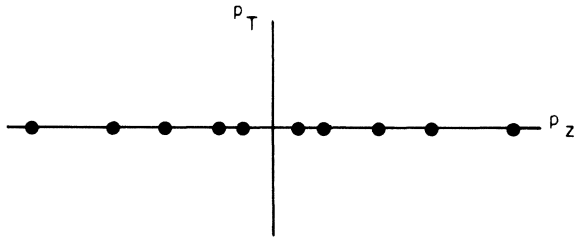


FIG. 1. Parton distributions in two colliding hadrons.

orders of magnitude in the kinematic range presently being explored in the Fermilab experiments.³ This is a surprising fact that we wish to emphasize here. It plays a significant role in explaining the unimportance of vector exchange in these processes.

This article is organized as follows. In Sec. II we review the calculation of high-momentum-transfer hadronic collisions in the naive parton model of Berman, Bjorken, and Kogut (BBK).⁶ Section III contains a short explanation of the physical picture underlying the AF⁷ and the scale-invariant parton models.⁸ In Sec. IV the physical picture discussed in Sec. III is used to generalize the naive parton model of BBK to include renormalizable field theories which might be either scale-invariant or AF at short distances. The resulting formulas are discussed semiquantitatively. In Sec. V numerical analysis of the differential cross section for the production of high-transverse-momentum hadrons is presented. The estimate for the AF parton model is compared with the naive-parton-model calculation. Curves of the differential cross sections are presented for Fermilab kinematic conditions. Related curves are presented and discussed. Section VI concludes with a discussion of results and related questions.

II. POINTLIKE PARTON MODEL FOR HADRON+HADRON→HADRON+X

First we shall review the calculation of large-momentum-transfer hadronic collisions assuming

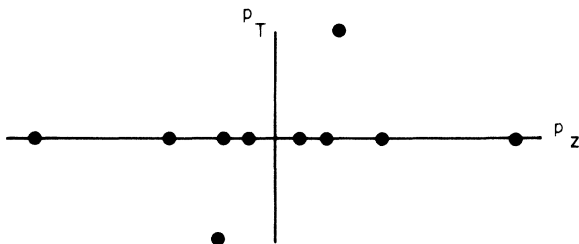


FIG. 2. Parton configuration immediately after a hard parton-parton collision.

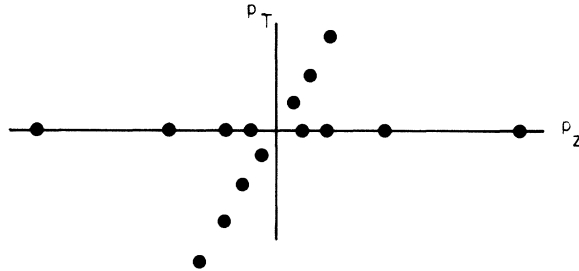


FIG. 3. Hadron configuration long after the hard collision.

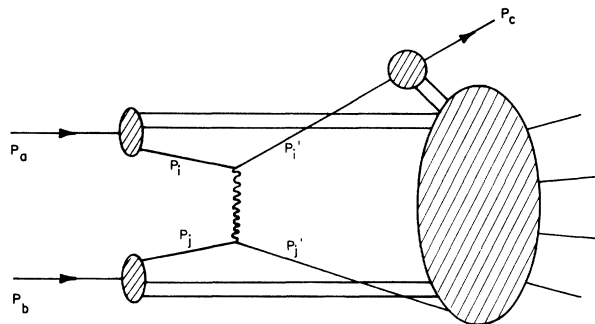
the validity of the pointlike parton model with single vector-gluon exchange.⁶ Consider the collision in the center-of-mass frame and let the beam direction be the z axis. View each hadron as a collection of partons each carrying a fraction x of the total momentum of the parent hadron (Fig. 1) and negligible transverse momentum. The probability dP_{ai} of finding a parton of type i carrying longitudinal fraction x is

$$dP_{ai} = \frac{F_{ai}(x)}{e_i^2} \frac{dx}{x}, \quad (2.1)$$

where the probability functions $F_{ai}(x)$ are measured in deep-inelastic lepton scattering off hadron a . For example, for electron scattering,

$$\nu W_2^{(a)}(x) = \sum_i F_{ai}(x). \quad (2.2)$$

As the hadrons pass by one another a vector meson is exchanged. Assuming that it carries large transverse momentum, one can calculate the exchange process in the impulse approximation, i.e., for the duration of the scattering process one treats the partons as quasifree. After the exchange two partons (the "active" ones in the scattering) find themselves with large transverse momenta (Fig. 2). The last ingredient in the calculation is to relate this configuration of partons to an equivalent configuration of hadrons. This is a

FIG. 4. Kinematics of a hard parton-parton collision between hadrons. The active partons are labeled i and j .

difficult problem which lies at the heart of the quark-confinement problem. However, on the basis of physical intuitions⁶ and various simple models,⁹ it has been suggested that the parton configuration of Fig. 2 evolves into the hadron configuration of Fig. 3. In more detail, each active parton gives rise to a jet of hadrons having predominantly low momentum transverse to the active parton's momentum. This distribution (jet) of hadrons is assumed to satisfy a scaling law in analogy to Eq. (2.1): The differential probability dP_{ic} of finding a hadron of type c associated with the active parton of type i and having fraction x of that parton's momentum is

$$dP_{ic} = G_{ic}(x) \frac{dx}{x}. \quad (2.3)$$

Various properties and the general shape of G_{ic} were obtained in Ref. 6. Furthermore, $\sum_i e_i^2 G_{ic}$ is directly measurable experimentally; it is just the inclusive hadron distribution in the annihilation process $e^+e^- \rightarrow$ virtual photon $\rightarrow h + X$.

Within this model, the differential cross section $d\sigma$ for $h + h \rightarrow h + X$ can now be calculated. The calculation consists of three parts (Fig. 4): first, the probability of finding partons within the parent hadrons; second, the differential cross section for the scattering of two active partons, $d\sigma(\text{parton})$,

by vector-gluon exchange; and, third, the probability that one of the active partons generates a hadron of large momentum transverse to the initial collision axis,

$$d\sigma = \sum_{i,j} \int \left[\frac{F_{ai}(x_i)}{e_i^2 x_i} dx_i \right] \left[\frac{F_{bj}(x_j)}{e_j^2 x_j} dx_j \right] \times d\sigma(\text{parton}) \left[\frac{G_{ic}(x)}{x} dx \right] + (i' \rightleftharpoons j'). \quad (2.4)$$

The differential cross section $d\sigma(\text{parton})$ is given by single gluon exchange. Finally one should rewrite Eq. (2.4) in a more convenient form. An exercise in kinematics which can be found in Ref. 6 allows Eq. (2.4) to be simplified to

$$E_c \frac{d\sigma}{dp_T^2 dp_a} = \frac{4\pi}{p_T^4} [\mathfrak{F}(x_1, x_2) + (1 \rightleftharpoons 2)], \quad (2.5)$$

where the dimensionless kinematic variables x_1 and x_2 are defined as

$$x_1 = -\frac{(p_b - p_c)^2}{(p_a + p_b)^2}, \quad x_2 = -\frac{(p_a - p_c)^2}{(p_a + p_b)^2}, \quad (2.6)$$

$$x_1 = -u/s, \quad x_2 = -t/s.$$

Finally,

$$\begin{aligned} \mathfrak{F}(x_1, x_2) &= \frac{1}{2} \left(\frac{g^2}{4\pi} \right)^2 \int \frac{x_1^2 (y_1^2 y_2^2 + x_1^2)}{y_1^4 (y_1 y_2 - x_1) y_2^2} \sum_i F_{ai}(y_1) G_{ic}(y_2) F_b \left(\frac{x_2 y_1}{y_1 y_2 - x_1} \right) dy_1 dy_2 \\ &= \frac{1}{2} \left(\frac{g^2}{4\pi} \right)^2 \int \frac{x_1^2 [(x_2 y_1 + x_1 y_1')^2 + x_1^2 y_1'^2]}{y_1^3 y_1' (x_2 y_1 + x_1 y_1')^2} \sum_i F_{ai}(y_1) G_{ic} \left(\frac{x_1}{y_1} + \frac{x_2}{y_1'} \right) F_b(y_1') dy_1 dy_1', \end{aligned} \quad (2.7)$$

where g is the quark-gluon coupling constant. Equation (2.5) has several important features. First is the scaling law, p_T^{-4} times a dimensionless function of dimensionless kinematic variables. The p_T^{-4} reflects, naturally, the exchange of a single vector gluon between quark partons. A second property, which proves important in practice, is that \mathfrak{F} receives most of its contribution from the region of integration where the arguments of the structure functions F and G are near 1, i.e., near the threshold regions.¹⁰ The reason for this follows from the fact that if one wants to produce a hadron of large transverse momentum, one needs active partons to collide with large relative subenergy. This requirement favors partons which carry large fractions of the momentum of the parent hadrons.

III. SCALE-INVARIANT AND AF PARTON MODELS

The naive parton model assumes that partons experience finite forces at short distances. In

particular, one assumes that the Hamiltonian describing parton dynamics consists of two terms, the first, H_0 , describing the kinetic energy of the quarks and gluons, and the second, H_{int} , describing the interactions between these quanta. Then

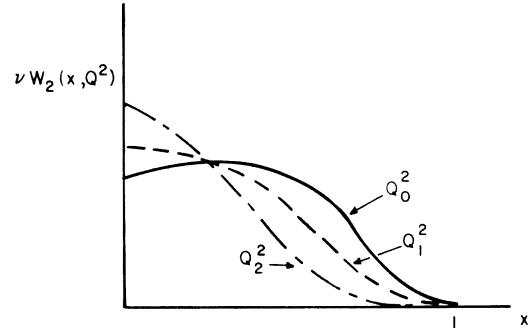


FIG. 5. Qualitative features of the Q^2 dependence of νW_2 . Each curve is labeled by a definite Q^2 , $Q_0^2 < Q_1^2 < Q_2^2$.

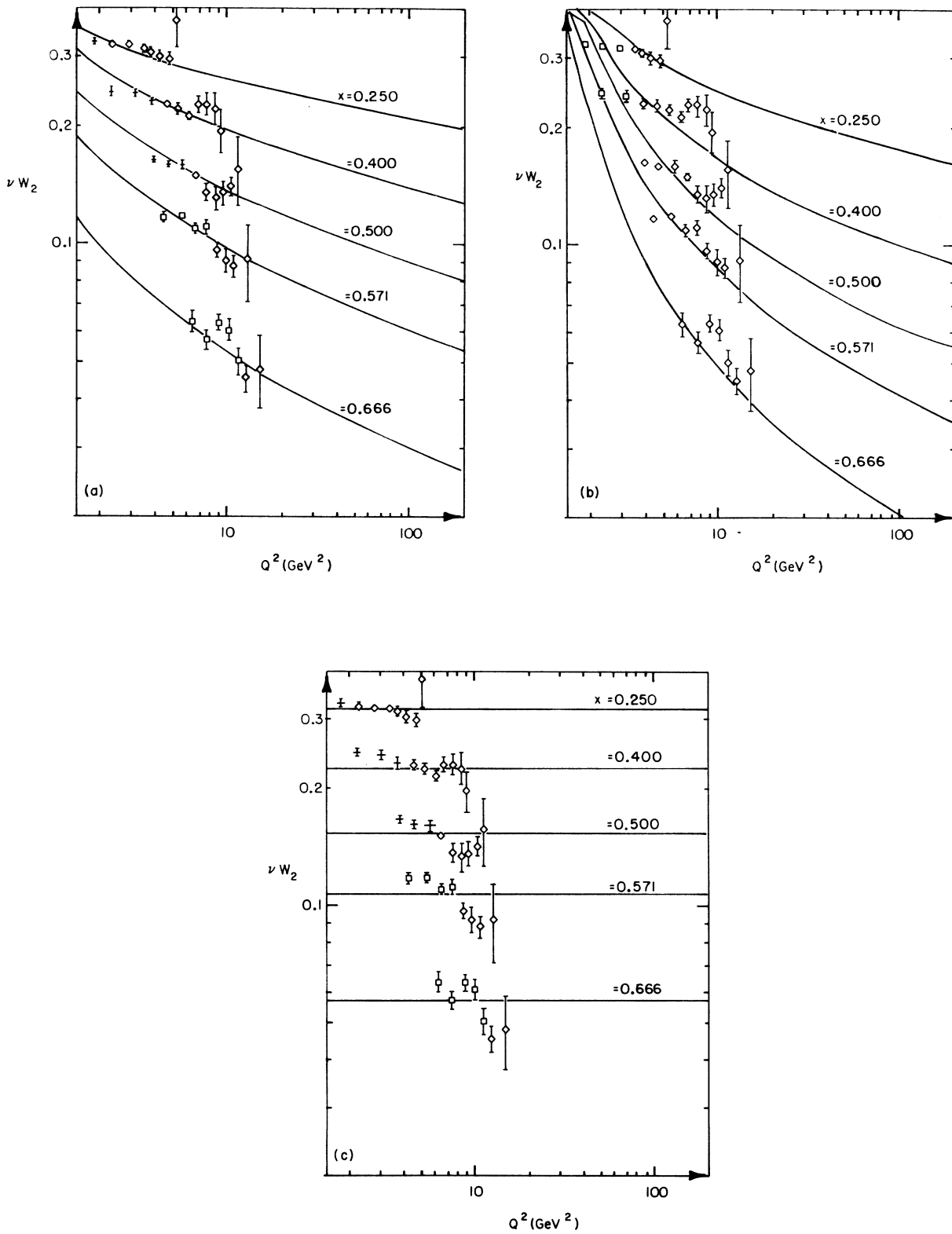


FIG. 6. (a) AF fit to data on νW_2 for the choice $\mu^2 = 0.2 \text{ GeV}^2$ in Eq. (4.6). Each line is labeled with its x value. (b) Same as (a) except $\mu^2 = 1 \text{ GeV}^2$. (c) Exact Bjorken scaling fits to the data.

one postulates that H_0 is much more significant in its action over short distances and times than H_{int} . This type of behavior is not generally shared by the familiar renormalizable field theories. Hence, there is good reason to generalize the parton-model approach to theories in which H_{int} is also important at short distances. This program was initiated and developed in a series of articles.^{7,8} We will review the physical pic-

ture behind it in order to generalize Eqs. (2.5) and (2.7) to interacting field theories.

Suppose that H_{int} is not negligible compared to H_0 . This then means that in general one cannot consider a hadron to be a collection of bare quanta. Rather, the quanta are dressed by the interactions and the concept of pointlike constituent no longer applies. Instead, the dressing of the quanta means that an external probe will

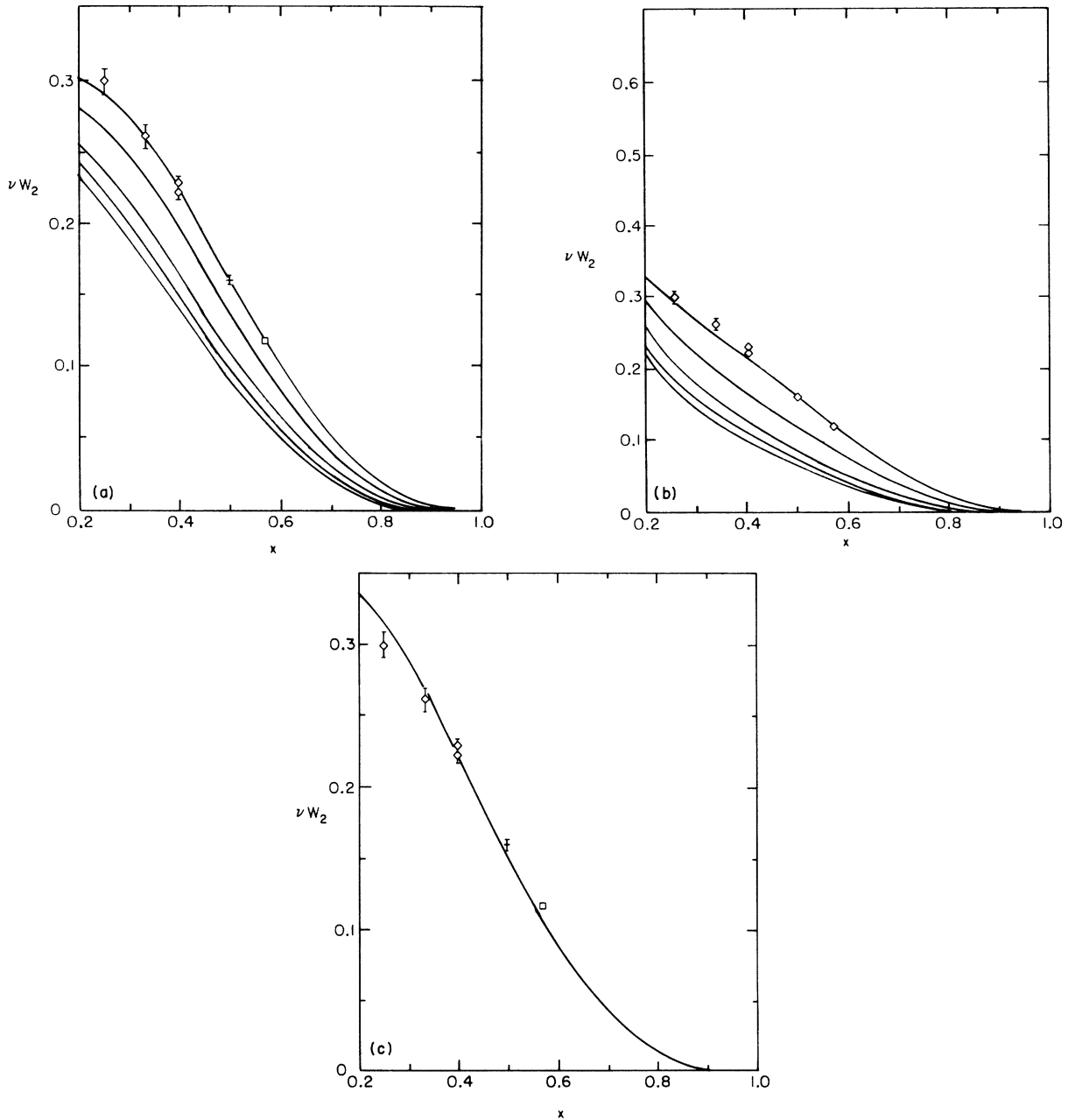


FIG. 7. (a) Breakdown of scaling following from Eq. (4.6) and the choice $\mu^2 = 0.2 \text{ GeV}^2$. The curves are at fixed $Q^2 = 5, 10, 30, 60,$ and 100 GeV^2 and arise from the same fit as in Fig. 6. The data points are at $Q^2 \approx 5 \text{ GeV}^2$. As Q^2 increases the curves fall for $x > 0.25$. (b) Same as (a) except $\mu^2 = 1 \text{ GeV}^2$. (c) Exact scaling fit to νW_2 .

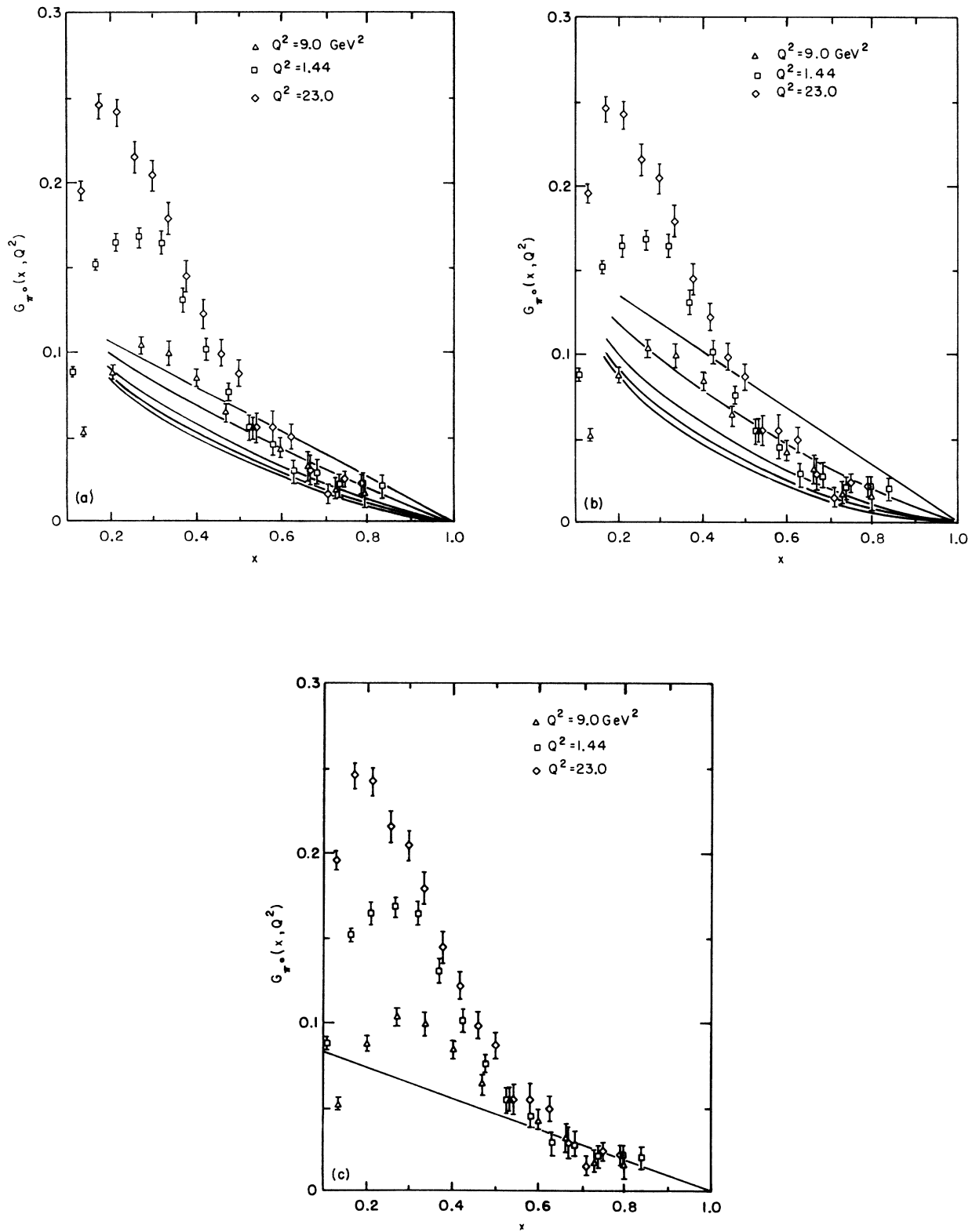


FIG. 8. (a) Analogous fits to Fig. 7(a) for inclusive hadron spectra measured at SPEAR. Q^2 values are again 5, 10, 30, 60, and 100 GeV^2 for $\mu^2 = 0.2 \text{ GeV}^2$ in Eq. (4.6). The fit includes the data only for $x > 0.50$. (b) Same as (a) except $\mu^2 = 1 \text{ GeV}^2$. (c) Exact scaling fit to the form $A_c(1-x)$.

uncover more and more structure within the hadron as its resolution is increased. Instead of pointlike constituents residing within the hadron, one must think of a hierarchy of constituents which vary in size from a fraction of the size of a hadron to zero. Now consider such a hadron in an infinite-momentum frame and suppose it absorbs a spacelike momentum transfer Q . This external probe will resolve transverse distances of order Q^{-1} . In particular, constituents of size larger than Q^{-1} will be broken up by the probe while constituents of lesser size will not be resolved by it. In fact, constituents of size of order Q^{-1} effectively absorb the external momentum transfer incoherently and allow the process to be described in a generalized parton-model fashion, i.e., $\nu W_2(x, Q^2)$ measures the longitudinal momentum distribution of charged constituents in the hadron of transverse extent $\sim Q^{-1}$. We have

$$\nu W_2^{(a)}(x, Q^2) = \sum_i F_{ai}(x, Q^2), \quad (3.1)$$

where $F_{ai}(x, Q^2)$ denotes the longitudinal momentum distribution of constituents of charge e_i and transverse size Q^{-1} .

The qualitative features of $\nu W_2(x, Q^2)$ can be easily understood from this physical picture. At

fixed $Q^2 = Q_0^2$, the external current measures the longitudinal momentum distribution of constituents of size $\sim Q_0^{-1}$. Now let Q^2 increase so that the spatial resolution of the probe increases. Then the constituents of size Q_0^{-1} will be resolved into smaller constituents of size Q^{-1} . However, the total longitudinal fraction of the smaller constituents of a constituent of size Q_0^{-1} must equal the longitudinal fraction of the parent constituent. Hence, $\nu W_2(x, Q^2)$ will be concentrated at smaller x values than $\nu W_2(x, Q_0^2)$, while the area under $\nu W_2(x, Q^2)$ equals the area under $\nu W_2(x, Q_0^2)$. Therefore, as Q^2 grows, $\nu W_2(x, Q^2)$ should vary as shown in Fig. 5.

More detailed properties of νW_2 can be obtained by developing the mathematical machinery behind the physical picture reviewed here. This has been done in Refs. 7 and 8 for both AF and scale-invariant field theories. One finds, in agreement with more formal approaches,¹¹ that the moments of νW_2 reflect the character of the short-distance interactions in the theory. For AF gauge theories one finds

$$\int_0^1 x^{\alpha-1} \nu W_2 dx \sim (\ln Q^2)^{-d_\alpha} M_\alpha, \quad (3.2)$$

where $d_1 = 0$ and $d_\alpha \sim \text{const} \times \ln \alpha$, as α becomes

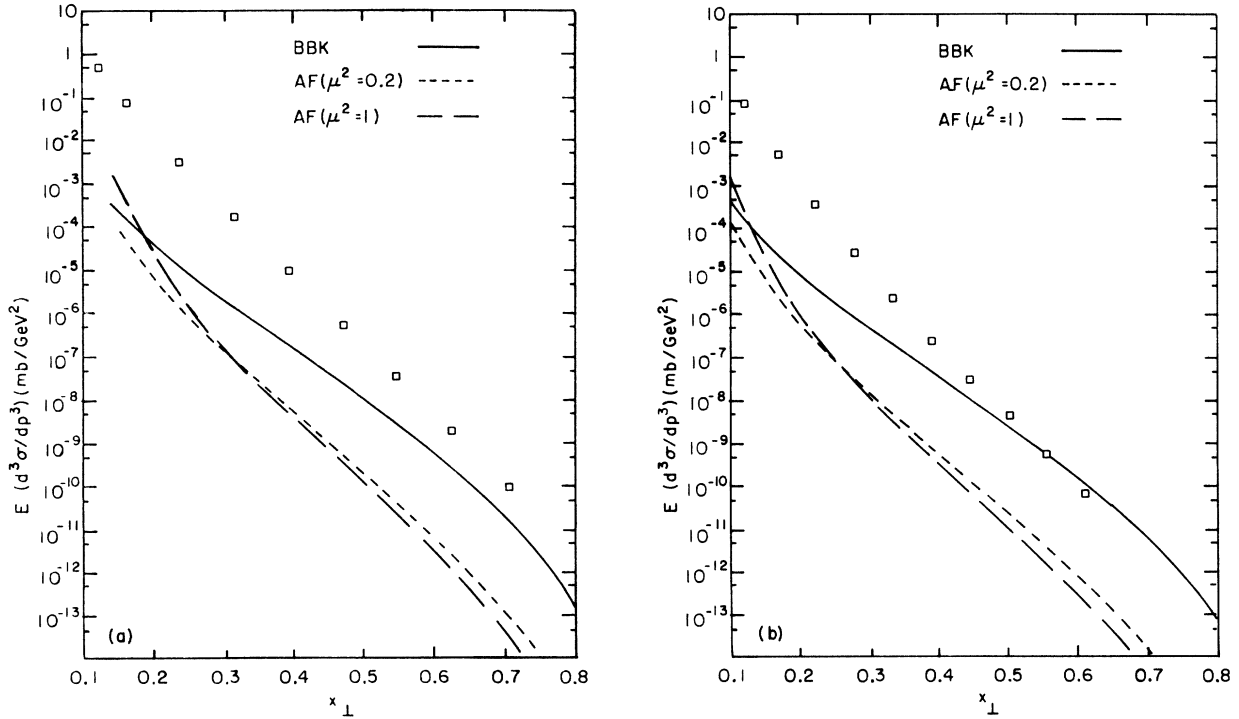


FIG. 9. (a) Differential cross sections as a function of x_\perp for $p_{\text{lab}} = 200$ GeV/c. The graph shows the Fermilab data points, the BBK predictions, and the AF predictions for $\mu^2 = 0.2$ and 1 GeV². The BBK curve has been normalized to the AF ($\mu^2 = 0.2$) curve at $x_\perp = 0.1$. (b) Same as (a) except $p_{\text{lab}} = 400$ GeV/c.

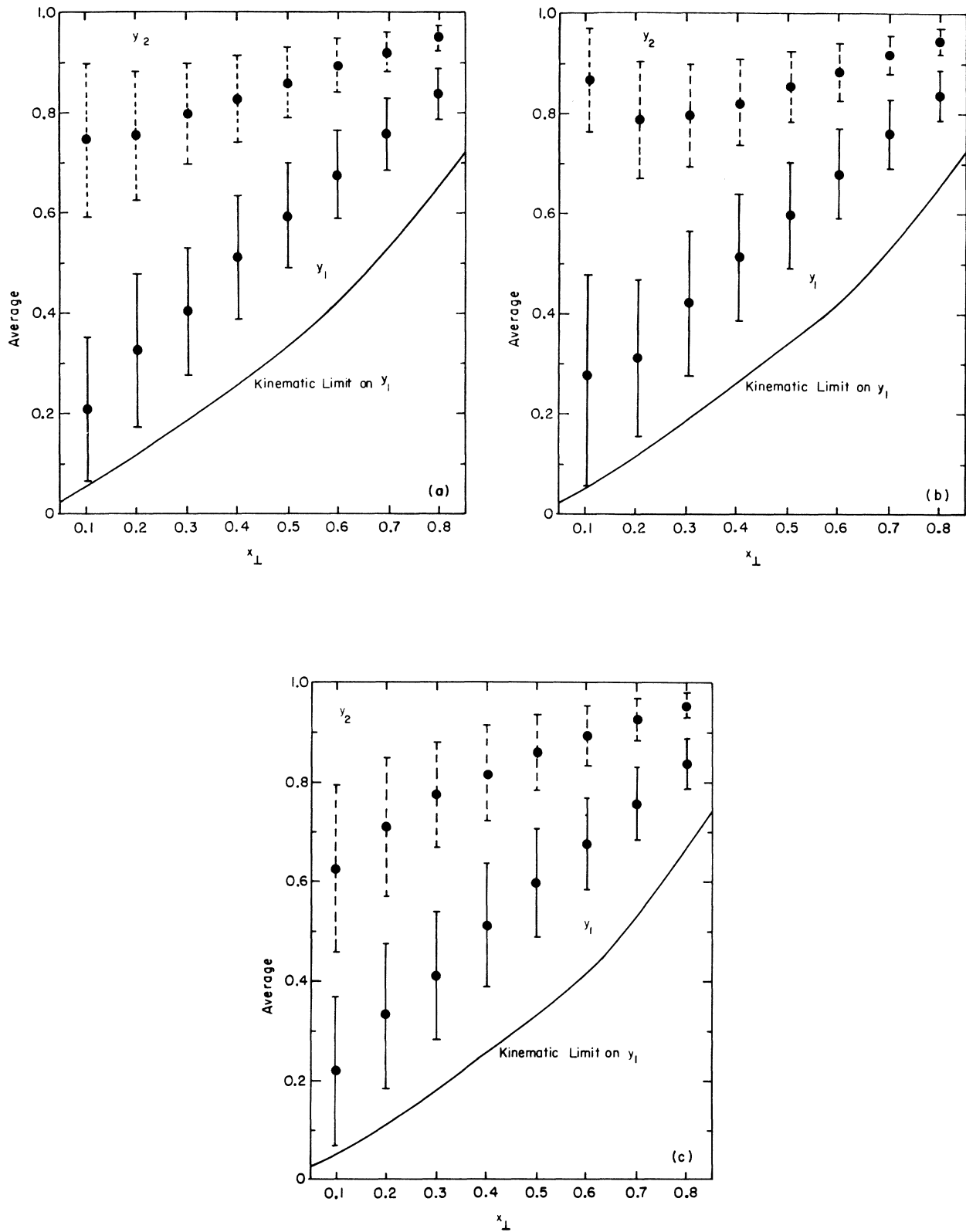


FIG. 10. (a) Mean values of y_1 and y_2 as a function of x_1 for AF($\mu^2=0.2$) curves at $p_{\text{lab}}=300$ GeV/c. (b) Same as (a) except $\mu^2=1$ GeV 2 . (c) Same as (a) except for BBK.

large. For scale-invariant interacting theories,

$$\int_0^1 x^{\alpha-1} \nu W_2 dx \sim (Q^2)^{-S} M_\alpha, \quad (3.3)$$

where $S_1 = 0$ and $S_i > S_{i-1}$. We note that these formulas suggest that the breakdown of naive scaling will be particularly dramatic near $x=1$. Even in the case of AF theories where the moments depend only logarithmically on Q^2 , the deviations from naive scaling could be numerically considerable near $x=1$ since the indices d_α grow logarithmically with α . This fact will play an important role in the estimates to follow.

IV. HADRON PRODUCTION AT LARGE p_T

Let us now reconsider Eq. (2.7) and Fig. 4 in theories which have non-negligible interactions at short distances. In particular, suppose that the vector gluon carries a momentum transfer Q . Then by direct analogy with the discussion of deep-inelastic scattering in Sec. III we realize that the parton distributions F_{at} of the naive pointlike theory must be replaced by the distribution $F_{at}(x, Q^2)$ of the constituents of size $\sim Q^{-1}$ in the interacting theories. Furthermore, the coupling constant $g^2/4\pi$ at the vector-gluon-quark constituent vertex must be replaced by the running coupling constant $\bar{g}^2(Q^2)/4\pi$ which characterizes the strength of interactions between constituents of the size Q^{-1} . The final modification of Eq. (2.7) rests in the function $G(x, Q^2)$ which represents the fragmentation function of the active parton of size Q^{-1} . Thus, $G(x, Q^2)$ is the inclusive distribution of hadrons produced in the annihilation reaction $e^+e^- \rightarrow \text{virtual photon} \rightarrow h + X$. More precisely,

$$p \frac{d\sigma_c}{d\Omega dp} = \frac{\pi^2 \alpha^2}{Q^2} (1 + \cos^2 \theta) \sum_i e_i^2 G_{ic}(x, Q^2), \quad (4.1)$$

where p is the total c.m. momentum of the detected hadron (of type c) and $x = 2p/(Q^2)^{1/2}$. Now we can collect these three ingredients and obtain the required generalization of Eqs. (2.5) and (2.7),

$$E_c \frac{d\sigma}{dp_T^2 dp_z} = \frac{4\pi}{p_T^4} [\mathcal{F}(x_1, x_2; s) + (1 \rightleftharpoons 2)], \quad (4.2)$$

where

$$\begin{aligned} \mathcal{F}(x_1, x_2; s) = & \frac{1}{2} \sum_i \int \left(\frac{\bar{g}^2(Q^2)}{4\pi} \right)^2 \frac{x_1^2 (y_1^2 y_2^2 + x_1^2)}{y_1^4 (y_1 y_2 - x_1) y_2^2} \\ & \times F_{at}(y_1; Q^2) G_{ic}(y_2; Q^2) \\ & \times F_b \left(\frac{x_2 y_1}{y_1 y_2 - x_1}; Q^2 \right) dy_1 dy_2, \end{aligned} \quad (4.3)$$

and here Q^2 denotes the momentum transfer carried by the vector gluon. Q^2 is easily related to the overall s of the process and the other kinematic variables in the problem,

$$Q^2 = \frac{y_1 x_2}{y_2} \quad s = \frac{y_1 x_2}{y_2} \frac{p_T^2}{x_1 x_2}. \quad (4.4)$$

Using Eqs. (4.2) and (4.3) we proceed to estimate high-transverse-momentum production for AF and scale-invariant field theories.

Consider in detail the AF colored-quark model. Let there be 9 quarks (red, white, and blue \mathcal{P} , \mathcal{X} , and λ quarks) coupled to 8 gauge bosons. This theory is AF with an invariant coupling constant,⁴

$$\frac{\bar{g}^2}{4\pi^2} \underset{t \rightarrow \infty}{\sim} \frac{4}{9t}, \quad t = \ln(Q^2/\mu^2). \quad (4.5)$$

The scale parameter μ is not predicted by low-order perturbation theory. It characterizes the length scale at which interactions become small. To understand the approximate scaling results of SLAC one chooses μ^2 to be small. We shall consider the possibilities $\mu^2 = 1$ and 0.2 GeV^2 in the numerical estimates. Next we must estimate the Q^2 dependence in the structure functions $F(x, Q^2)$. As discussed in the Introduction and as can be verified numerically, Eq. (4.3) is sensitive only to the behavior of the structure functions near $x=1$ if we confine our attention to secondary hadrons of

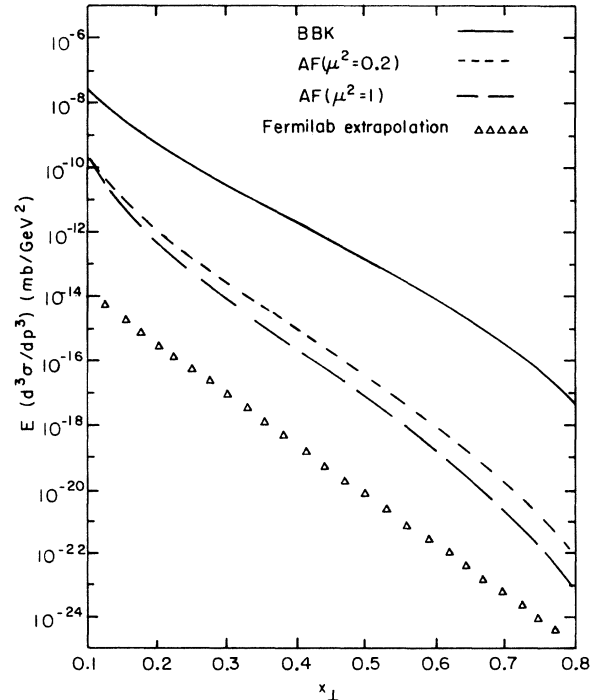


FIG. 11. Same as Fig. 9(a) except $s = 10^5 \text{ GeV}^2$ and Fermilab fit has been extrapolated.

considerable transverse momenta. So, we shall be satisfied with a reliable estimate of $F_{at}(x, Q^2)$ for $x \geq 0.50$, say. For AF theories such an estimate can be made in closed form. Suppose that the structure function is known exactly at some $Q^2 = Q_0^2$. Then the moments Eq. (3.2) allow one to obtain the structure function for any $Q^2 > Q_0^2$ given the indices d_α . Using methods first presented by Parisi,¹² and making various smoothness assumptions, this exercise has been done for the AF theory of interest here,¹³

$$\nu W_2(x, t) \approx \left(\frac{t}{t_0}\right)^{0.69G} \frac{6}{\Gamma(4+p)} (-\ln x)^p \nu W_2(x, t_0), \quad (4.6)$$

where

$$G = \frac{4}{27}, \quad p = 4G \ln(t/t_0)$$

and Eq. (4.6) is accurate for large x ($x > 0.50$). In the numerical estimates below we shall choose t_0 in the SLAC kinematic range ($Q_0^2 = 5 \text{ GeV}^2$). Before proceeding, however, it is instructive to estimate the amount of scale breaking contained in Eq. (4.6) over the kinematic range of interest to us.¹³ Let $\mu = 1 \text{ GeV}$ and compare $Q_0^2 = 5 \text{ GeV}^2$ with $Q^2 = 50 \text{ GeV}^2$,

$$\nu W_2(x, \ln 50) \approx \frac{1}{2} (\ln x)^{1/2} \nu W_2(x, \ln 5). \quad (4.7)$$

The important values of x in our calculation lie near 1. Consider $x = \frac{3}{4}$, for which $(\ln x)^{1/2} \approx \frac{1}{2}$. Hence, the scale-breaking effects in Eq. (4.3) coming just from the structure functions F_{at} and F_b can give a 16 to 1 reduction from naive scaling. This is surprisingly large effect. In addition, the coupling constant's Q^2 dependence further diminishes Eq. (4.3). In fact, comparing $Q^2 = 50 \text{ GeV}^2$

with $Q^2 = 5 \text{ GeV}^2$, we have another relative suppression factor of

$$\left(\frac{\bar{g}^2(50)/4\pi}{\bar{g}^2(5)/4\pi}\right)^2 = \left(\frac{\ln 5}{\ln 50}\right)^2 \approx 0.17, \quad (4.8)$$

which is also considerable. So, from these two effects we can expect a suppression of high-transverse-momentum hadrons by 1 to 2 orders of magnitude relative to the corresponding naive parton-model calculation. This will be confirmed by a numerical evaluation of Eq. (4.3) to be discussed below. The final ingredient in Eq. (4.3) is the Q^2 -dependent fragmentation function $G_{ic}(x, Q^2)$. Considerably less is known about $G_{ic}(x, Q^2)$ than $\nu W_2(x, Q^2)$. However, for scale-invariant theories it has been argued by Polyakov¹⁴ and confirmed by formal arguments¹⁵ that G should behave similarly to νW_2 , i.e., G should fall near $x=1$ and rise near $x=0$ as Q^2 grows. For x near 1 it is also reasonable to expect G to vary with Q^2 at the same rate as νW_2 does near $x=1$. Therefore, in our estimate we shall use Eq. (4.6) to estimate the expected scale breaking in G . Finally we must assume an initial value for G , say $G(x, 5 \text{ GeV}^2)$. Naive parton arguments contained in Ref. 6 suggested

$$G_{ic}(x, 5 \text{ GeV}^2) = A_c(1-x), \quad (4.9)$$

which we shall assume. The constant A_c will be obtained from the inclusive distributions measured at SPEAR¹⁶ for $x > 0.6$. Luckily, hadron production at large transverse momentum is sensitive only to $G(x, Q^2)$ near $x=1$. Therefore, our calculation is *not* affected by the excess of slow c.m. secondaries observed at SPEAR.¹⁶

Finally, we collect all these ingredients and evaluate Eq. (4.3) for AF theories,

$$\begin{aligned} \mathcal{F}(x_1, x_2; s) = & \frac{1}{2} \sum_i \int \frac{x_1^2 (y_1^2 y_2^2 + x_1^2)}{y_1^4 (y_1 y_2 - x_1) y_2^2} \left(\frac{\ln(Q^2/\mu^2)}{\ln(Q_0^2/\mu^2)} \right)^{2 \cdot 1G} \left(\frac{4\pi}{9 \ln(Q^2/\mu^2)} \right)^2 \left(\frac{6}{\Gamma(4+p)} \right)^3 \left[-\ln \left(\frac{x_2 y_1}{y_1 y_2 - x_1} \right) \ln y_1 \ln y_2 \right]^p \\ & \times F_b \left(\frac{x_2 y_1}{y_1 y_2 - x_1}; Q_0^2 \right) F_{at}(y_1; Q_0^2) G_{ic}(y_2; Q_0^2) dy_1 dy_2. \end{aligned} \quad (4.10)$$

V. NUMERICAL RESULTS

In this section we present numerical results based on partons with asymptotically small gluon interaction and consequent scale breaking described approximately by Eq. (4.6). First we examine the structure functions obtained from lepton-induced reactions in the region of $Q_0^2 \sim 5 \text{ GeV}^2$. This provides the normalization for the high- p_T distributions in hadron collisions. Then we compare the data on $pp \rightarrow \pi X$ with both the original parton model (BBK) and one incorporating

asymptotic freedom (AF). Next we extract an "effective power" of p_T from the model in order to simply describe its energy dependence. Finally, we consider $pp \rightarrow \pi X$ at $s = 10^5$ in the AF model.

The deep-inelastic experiments at SLAC have recently reported improved Q^2 resolution in the range $2 < Q^2 < 15$.¹⁷ Scale breaking at such relatively small Q^2 can still be absorbed into some residual mass dependence in one's choice of a scaling variable. Instead, we take it to be a real effect and accordingly apply the AF form, Eq. (4.6), readjusting the parameters of the usual

polynomial

$$F_2(x, Q_0^2 = 5) = a(1-x)^3 + b(1-x)^4 + c(1-x)^5.$$

The results are shown in Figs. 6(a) and 6(b) for $\mu^2 = 0.2$ and 1.0. The Q^2 dependence in the data is excellently accounted for, especially for $x > 0.50$, where Eq. (4.6) supposedly becomes reliable. The consequent distributions in x up to $Q^2 = 100 \text{ GeV}^2$ are given in Fig. 7 along with the Q_0^2 data for reference. Also included in Figs. 6(c) and 7(c) are fits which assume exact Bjorken scaling.

The colliding-beam results are more difficult to interpret due to a strongly Q^2 -dependent excess of slow hadrons ($x \lesssim 0.5$).¹⁶ Since the present model is sensitive only to the high-energy "tails" of this effect ($x \gtrsim 0.5$), we concentrate only on the high- x data in normalizing G . The raw data give the inclusive distribution for $e^+e^- \rightarrow$ charged hadron $+X$. The fast ($x \gtrsim 0.5$) hadrons are supposedly pions.¹⁶ To deduce the distribution for π^0 's we assume that the inclusive distributions for π^+ , π^- , and π^0 are roughly equal for $x \gtrsim 0.5$. Now one can obtain the constant A_{π^0} of Eq. (4.9) from the data,

$$G_{\pi^0}(x; 5 \text{ GeV}^2) \cong \frac{1}{3} \sum_a G_{\pi^0 a}(x; 5 \text{ GeV}^2) \cong 0.13(1-x). \quad (5.1)$$

Figures 8(a) and 8(b) show how the formula compares with the SPEAR data¹⁶ for $x \gtrsim 0.5$ and how the scale breaking of Eq. (4.6) distorts $G_{\pi^0}(x, Q^2)$ at higher Q^2 . Figure 8(c) shows the fit of Eq. (5.1) to the preliminary SPEAR data.

Next we evaluate Eq. (4.10) for two Fermilab energies (200 and 400 GeV) and compare with the data in Figs. 9(a) and 9(b). This plot shows the differential cross section as a function of $x_\perp = 2p_T/\sqrt{s}$ for secondary hadrons, which are produced at $\approx 90^\circ$ in the center-of-mass system. This corresponds to the choice of variables $x_1 = x_2 = x_\perp$ in the notation of Eq. (4.2). The naive-parton-model curve in Fig. 9(a) was normalized to agree with the AF prediction at $x_\perp = 0.1$ and $\mu^2 = 0.2 \text{ GeV}^2$. We note that the BBK curve crosses the data at $p_{\text{lab}} = 400 \text{ GeV}$, while the scale breaking in the AF curve bends it far below the data.

It was stated in Secs. I and IV that the yield of high-transverse-momentum hadrons depends sensitively on the behavior of the structure functions near $x=1$. We confirm this by plotting in Fig. 10 the average y_1 and y_2 for given x_\perp at Fermilab conditions ($p_{\text{lab}} = 300 \text{ GeV}$). Here y_1 and y_2 are the arguments in $F_{2i}(y_1; Q^2)$ and $G_{ic}(y_2; Q^2)$ appearing in Eq. (4.3) and (4.10). Note that $\langle y_2 \rangle$ is very near 1 for any choice of x_\perp while $\langle y_1 \rangle$ is greater than 0.5 (roughly) when $x_\perp > 0.4$. Since the estimate

of scale breaking in Eq. (4.6) is only reliable for $y_1 \gtrsim 0.5$, we should concentrate only on the region $x_\perp > 0.4$ in the curves of high-transverse-momentum hadronic cross sections shown in Figs. 9 and 12.

It is interesting to ask whether the AF curves will ever exceed a reasonable extrapolation of the Fermilab data to higher energies. Let us extrapolate the Fermilab fit,³

$$E \frac{d\sigma}{dp_\perp^2 dp_z} = \frac{\text{const}}{s^{5.4}} e^{-36x_\perp}, \quad (5.2)$$

to $s = 10^5 \text{ GeV}^2$ (an energy characteristic of presently proposed accelerators of the next generation) and compare with the BBK and AF curves at the energy. The results are shown in Fig. 11. We see that over the entire range of x_\perp the AF curves lie at least two orders of magnitude *above* Eq. (5.2). Of course, the absolute magnitudes of the cross sections are very small at these energies and momentum transfers.

It is interesting and convenient to summarize the scale-breaking effects in the AF curves through an index $n(x_\perp, s)$ which is defined through the fit

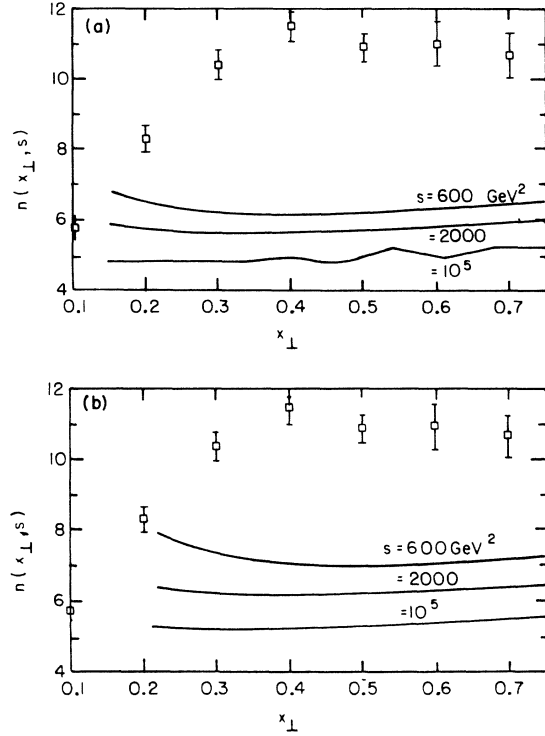


FIG. 12. (a) The index $n(x_\perp, s)$ as a function of x_\perp for AF curves with $\mu^2 = 0.2 \text{ GeV}^2$ at $s = 600, 2000,$ and 10^5 GeV^2 . The data points come from Fermilab fits at $s = 600 \text{ GeV}^2$. (b) Same as (a) except $\mu^2 = 1 \text{ GeV}^2$.

$$E \frac{d\sigma}{dp_T^2 dp_z} \approx (p_T)^{-n(x_\perp, s)} \times (\text{function of } x_\perp). \quad (5.3)$$

The naive parton model would have $n(x_\perp, s) = 4$, but the scale breaking of AF leads to larger values of $n(x_\perp, s)$ as shown in Figs. 12(a) and 12(b). Note that as s is increased to 10^5 GeV^2 , $n(x_\perp, s)$ falls to about 5.5. The fact that n decreases as s increases is easily understood since as s grows, the running coupling constant decreases and the scale breaking becomes smaller and smaller.

Finally, we consider the extrapolation of our curves to enormous energies somewhat more systematically. In Figs. 13(a) and 13(b) we plot BBK, AF, and Eq. (5.2) values as functions of s for $x_\perp = 0.4$ and 0.8 , respectively. Note that the AF curves cross Eq. (5.2) at $s \approx 6000 \text{ GeV}^2$ for $x_\perp = 0.4$. The differential cross section is about $10^{-12} \text{ mb/GeV}^2$ at that point. The prospects for measuring such a small differential cross section at such a large energy seem quite dim.

VI. DISCUSSION

The quantitative analysis of Sec. V supports our claim in the Introduction that single vector-gluon

exchange does not contribute significantly to wide-angle hadronic collisions in AF theories. We have seen that both the smallness of the invariant coupling constant and the scale breaking in these theories are the sources of our results. Thus, these theories evade the problems that naive theories of vector exchange have in discussing the energy and angular dependence observed in wide-angle hadron scattering processes. This result applies to inclusive reactions analyzed in detail here and also to exclusive processes. The reader can convince himself of this second claim by consulting Ref. 10. Here it is shown that even if $g^2/4\pi$ is about unity, the vector-gluon-exchange contribution to exclusive scattering lies below the data.

There are several potentially interesting effects which we have not included in our analysis. First, there are contributions to wide-angle scattering arising from hard-vector-gluon exchange between the gluon distributions within the colliding hadrons. Most theorists would guess that the gluon distribution is more concentrated near $x = 0$ than the distribution of \mathcal{O} quarks in a proton. If the gluon distribution lies below the quark distributions for $x \gtrsim 0.5$, then we are justified in ignoring them for $x_\perp \gtrsim 0.4$. Otherwise they may change our esti-

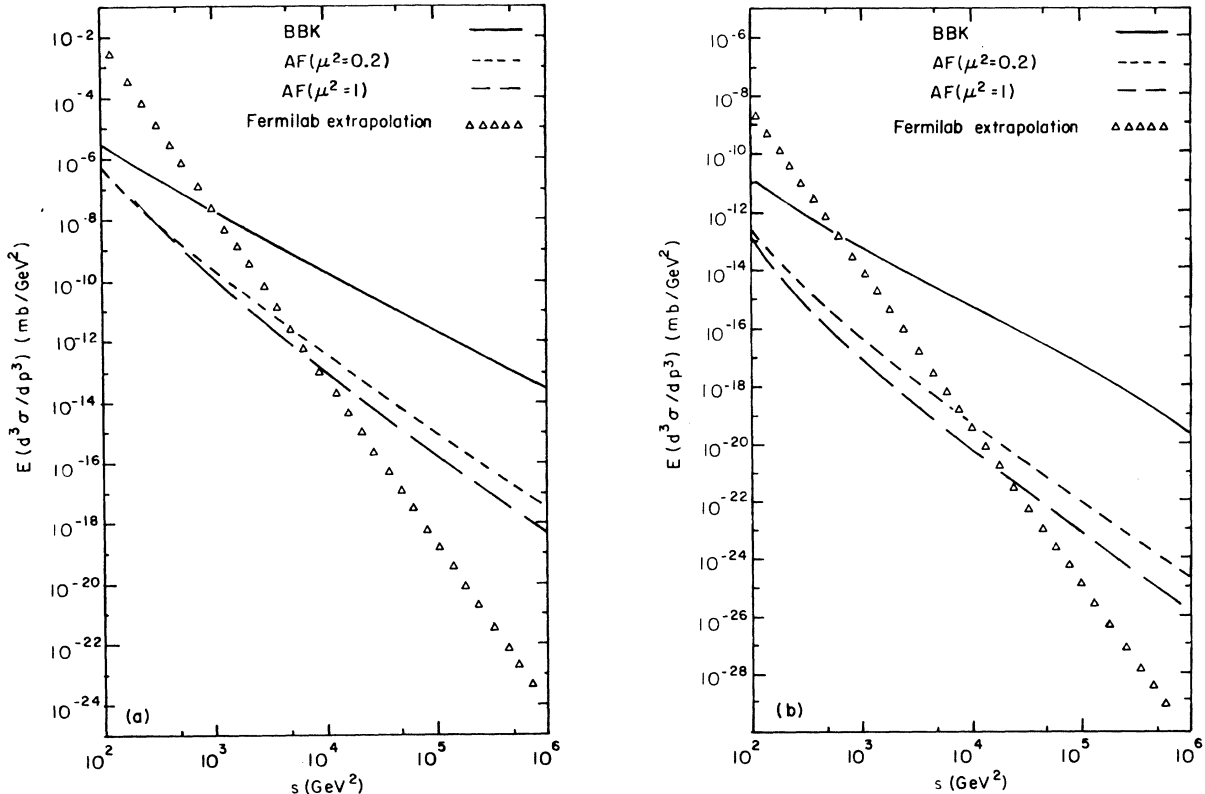


FIG. 13. (a) Differential cross sections as a function of s for $x_\perp = 0.4$. (b) Same as (a) except $x_\perp = 0.8$.

mates by a factor of 2 or 3, say. However, their contribution to wide-angle scattering will be affected by the smallness of $\bar{g}^2(Q^2)$ and scale breaking in the same way as estimated here for the quark distributions. Second, the hadronic "jet" resulting when a cluster of size $\sim Q^{-1}$ is struck by an exchanged vector gluon is expected to have a width in momentum space which grows with Q^2 . In particular, the mean squared momentum transverse to the direction of the struck cluster^{7,8} is of order $\sim \bar{g}^2(Q^2)Q^2$. The magnitude of this effect will be most clearly measured in studies of the final states of deep-inelastic processes.⁷ Once these data are available they can be used in calculations of wide-angle $h + h \rightarrow h + X$. Its effect on wide-angle scattering is difficult to estimate on purely theoretical grounds since the estimate involves an understanding of the composite structure (wave function) of hadrons. However, if the detected hadron in $h + h \rightarrow h + X$ has sufficiently high p_T , there is little energy available to other secondaries to fan the jet out significantly. For these events our estimates should be accurate. In general a more careful analysis armed with data on the final states of deep-inelastic scattering is necessary.

Of course, our calculations do not answer the primary question: What is the source of the high-transverse-momentum collisions observed at CERN ISR and Fermilab? Presumably the dynamics behind the data does not rely on vector-gluon-quark coupling (\bar{g}^2 is too small at large Q^2) or simple exchange mechanisms (they are suppressed by scale breaking). This suggests that high-transverse-momentum hadrons are produced by successive subscatterings, each of relatively moderate momentum transfer, of constituents within the colliding hadrons. Such mechanisms should blend in smoothly with Regge exchange at low p_T as the data apparently do. Of

course, if this is true, then purely hadronic high-transverse-momentum processes are complicated and not too revealing.

A highly developed model of wide-angle hadronic processes which does not rely on gluon coupling or exchange processes has been presented by Brodsky, Blankenbecler, and Gunion.¹⁸ It would be interesting to know if such a bound-state picture occurs in AF theories and how severely scale breaking changes the model's predictions. These are interesting questions for study.

We also noted in Fig. 13 that single vector exchange in AF theories will dominate the extrapolation of the Fermilab data to values of s in the neighborhood of 6000 GeV². However, the cross sections are so small for these momentum transfers that they will probably either be dominated by other processes or be below the rate restrictions of accelerators.

Note added in proof: After the first draft of this article was prepared we learned from J. Gunion that he has considered the AF modifications to the interchange theory (J. Gunion, unpublished).

ACKNOWLEDGMENT

The authors thank their colleagues at Syracuse and Cornell for discussions. Two of us (J. K. and L. S.) also thank S. Brodsky for emphasizing to us repeatedly that the present data on wide-angle hadron scattering show no evidence for vector exchange. The authors also thank A. De Rújula for a helpful discussion of scale breaking in AF field theories. Finally, K. Geer thanks the Theory Group of the High Energy Physics Division of Argonne National Laboratory, and R. Cahalan thanks the Aspen Center for Physics for their hospitality and support during a portion of this research.

*Work supported in part by the U. S. Atomic Energy Commission.

†On leave of absence to Institute for Nuclear Research, Warsaw, Poland.

‡Present address: Physics Dept., Ohio State University, Columbus, Ohio 43210.

§Work supported in part by the National Science Foundation.

|| Work supported by NSF Grant No. GP-38863.

¶Present address: Tel Aviv University, Ramat Aviv, Tel Aviv, Israel (Permanent address: Yeshiva University, New York, N. Y. 10013).

¹T. T. Wu and C. N. Yang, Phys. Rev. **137**, B708 (1965).

²For example, T. T. Chou and C. N. Yang, Phys. Rev. **170**, 1591 (1968); Phys. Rev. Lett. **20**, 1213 (1968);

H. D. I. Abarbanel, S. D. Drell, and F. J. Gilman, *ibid.* **20**, 280 (1968); Phys. Rev. **177**, 2458 (1969). More recently S. M. Berman and M. Jacob, Phys. Rev. Lett. **25**, 1683 (1970).

³C. M. Ankenbrandt *et al.*, Phys. Rev. **170**, 1223 (1968); F. W. Büsser *et al.*, Phys. Lett. **46B**, 971 (1973); J. Cronin *et al.*, Phys. Rev. Lett. **31**, 1426 (1973).

⁴G. 't Hooft, 1972 (unpublished); H. D. Politzer, Phys. Rev. Lett. **30**, 1346 (1973); D. J. Gross and F. Wilczek, *ibid.* **30**, 1343 (1973). For an SU(3)' octet of gauge bosons $b_0 = \frac{3}{2}$.

⁵J. D. Bjorken, Phys. Rev. **179**, 1547 (1969).

⁶S. M. Berman, J. D. Bjorken, and J. B. Kogut, Phys. Rev. D **4**, 3388 (1971).

⁷J. Kogut and Leonard Susskind, Phys. Rev. D **9**, 3391

- (1974).
- ⁸J. Kogut and Leonard Susskind, *Phys. Rev. D* 9, 697 (1974).
- ⁹A. Casher, J. Kogut, and Leonard Susskind, *Phys. Rev. Lett.* 31, 792 (1973).
- ¹⁰S. D. Ellis and M. B. Kislinger, *Phys. Rev. D* 9, 2027 (1974).
- ¹¹G. Mack, *Nucl. Phys.* B35, 592 (1971); N. Christ, B. Hasslacher, and A. Mueller, *Phys. Rev. D* 6, 3543 (1972); D. J. Gross and F. Wilczek, *ibid.* 8, 3633 (1973); H. Georgi and H. D. Politzer, *ibid.* 9, 416 (1974).
- ¹²G. Parisi, *Phys. Lett.* 43B, 207 (1973); 50B, 367 (1974).
- ¹³D. J. Gross, *Phys. Rev. Lett.* 32, 1071 (1974).
- ¹⁴A. M. Polyakov, *Zh. Eksp. Teor. Fiz.* 60, 1572 (1971) [*Sov. Phys.—JETP* 33, 850 (1971)].
- ¹⁵A. Mueller, *Phys. Rev. D* 9, 963 (1974).
- ¹⁶B. Richter, invited talk at the American Physical Society meeting, Chicago, 1974 (unpublished).
- ¹⁷A. Bodek *et al.*, *Phys. Lett.* 52B, 249 (1974).
- ¹⁸J. F. Gunion, S. J. Brodsky, and R. Blankenbecler, *Phys. Lett.* 39B, 649 (1972).